Dalton Transactions

Accepted Manuscript

ROYAL SOCIETY OF CHEMISTRY

www.rsc.org/dalton

Journal Name

RSCPublishing

ARTICLE

Heterobimetallic catechol-phosphine complexes with palladium and a group-13 element: structural flexibility and dynamics

Cite this: DOI: 10.1039/xoxxooooox

Received ooth January 2012,
Accepted ooth January 2012

DOI: 10.1039/xoxxooooox

www.rsc.org/

G. Bauer,[a] M. Nieger[b] and D. Gudat[a]

Group-13 metal acetylacetonates [M(acac)$_3$] (M = Al, Ga, In) or Al(OiPr)$_3$ react with a complex [Pd(catphosH)$_2$}] that may act as chelating ligand towards a second metal, or with a mixture of catechol phosphine (catphosH$_2$) and [PdCl$_2$(cod)], to give heterometallic complexes featuring either dinuclear M(catphos)$_2$Pd or trinuclear M{(catphos)$_2$Pd}$_2$ motifs. Characterisation of the products by crystallographic and solution NMR studies gives insight into the structural diversity and flexibility of the coordination environments of the group-13 elements and their impact on the stability of the multinuclear complexes. The results indicate that gallium and indium are the most suitable elements for the stabilisation of di- and trinuclear assemblies, respectively. Dynamic NMR spectroscopy allowed to follow the dynamic averaging of the coordination environments of the four distinguishable catechol phosphines in the indium complex [M{(catphos)$_2$Pd}$_2$]H. The results revealed that the isomerisation follows a complex pathway involving several distinguishable proton transfer steps, and allowed to propose a mechanistic explanation for the observed isomerisation.

Introduction

Functional phosphines with additional, electronically different coordinating groups receive persistent attention as hybrid ligands for uses in coordination chemistry and catalysis.[1] For instance, hydroxyphosphines [2] combine a phosphorus atom, which is generally considered a "soft" donor centre, with one or several alcohol or phenol moieties that can serve as neutral or (after deprotonation) anionic "hard" metal binding sites. If the molecular backbone permits to connect electronically different functions with the same metal atom, such ligands can form chelate complexes which may have potential applications in catalysis.[1,2] However, the dissimilar binding preferences of the coordinating groups can as well be used to direct metal atoms specifically to the hard (O) and soft (P) donor site. This feature enables to control the ambident behaviour of hydroxy-phosphines in mononuclear complexes, but permits to employ such ligands also as smart building blocks for the selective assembly of heterometallic complexes. Particularly illustrative examples have been reported for ditopic catechol phosphines like **1**, which was used as platform for larger supramolecular architectures,[3] or **2**, which forms a scaffold for the construction of defined heterometallic complexes of type **A** (e. g. with M' = Pd, Pt and M(L)$_n$ = MoO$_2$, WO$_2$, VO,[4] or M(L)$_n$ = GaCl, SnCl$_2$, BiCl [5]) and **B** (M(L)$_n$ = Zr, x = 0 [5] or M(L)$_n$ = Y(DMF), x = 1;[6] Scheme 1). The terminal oxygen atoms of catecholate ligands in **A** and **B** still exhibit some basicity which allows them to act as hydrogen bond acceptors [4] or undergo protonation.[6]

Interestingly, it was found that the bite angle of the multidentate array varies with the size and preferred coordination geometry of the template, and the choice of suitable templates from different groups of the periodic table allowed thus to construct e. g. *trans*-chelating bisphosphine moieties with bite angles close to 180° [7] and *cis*-chelating bisphosphine units with bite angles between 102° to 97° [5] from the same catechol phosphine building block. The P$_2$O$_2$ donor set around the Pd atom in type **A** complexes shows hemilabile behaviour, and some complexes were found to exhibit catalytic activity in CC cross-coupling reactions.[5]

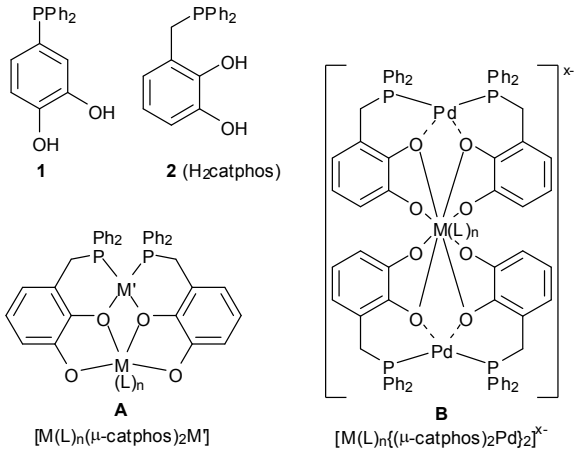

Scheme 1 Molecular structures of catechol phosphine ligands **1**, **2** (= H_2catphos) and complexes $[M(L)_n(\mu\text{-catphos})_2M']$ (**A**) and $[M(L)_n\{(\mu\text{-catphos})_2Pd\}_2]^{x-}$ (**B**).

The synthesis of the oligonuclear complexes **A**, **B** can be either accomplished in a single step by spontaneous condensation of ligand **2** with two simple metal salts,[5,6] or stepwise by introducing the metal atoms one after the other (Scheme 2).[4,7] In the sequential reactions, the first metal atom interacts with one coordination site of two catechol phosphines to produce complexes of types **C** or **D**, respectively, which then act as bi- or multidentate donors towards a second metal atom. Since the coordinative bonds between the catechol phosphine and the metal template are kinetically labile and their formation is in principle reversible, complexes **C**, **D** were also denoted supramolecular ligands.[4,5]

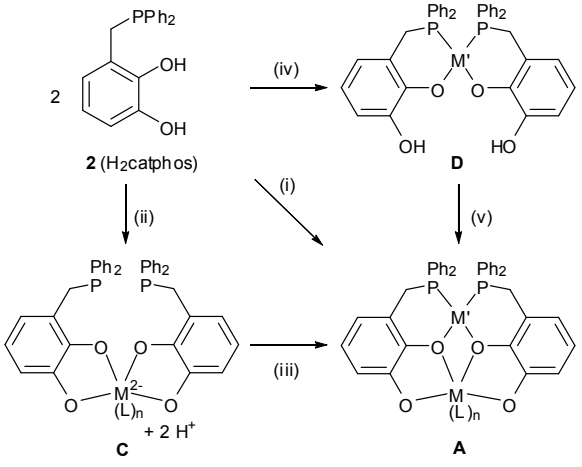

Scheme 2 Synthetic approaches to heterometallic complexes **A**

In this work, we report on the outcome of a systematic survey of heterometallic complexes containing palladium and a group-13 element. The results provide additional insight into the structural flexibility and dynamics of the template-centred multidentate donor units, and cast some light on the factors that govern the aggregation of individual ligating units.

Results and Discussion

Syntheses.

Examples of complexes **A** with group-13 elements are as yet known with boron ($M(L)_n$ = B; M' = Cu(I), Ag(I), Au(I))[7] and gallium ($M(L)_n$ = GaCl; M' = Pd(II)).[5] The total cation charge in these species is, like in all other previously prepared type **A** complexes, four or larger. Since at the same time attempts to prepare anionic complexes with lower cation charges failed,[8] it seems that formation of a stable bimetallic framework requires a high electrostatic contribution to the metal-ligand bonding, and we consider the use of trivalent group-13 cations therefore an essential prerequisite for successful synthesis of the target compounds. As thallium exhibits a strong preference for the +I-oxidation state and Tl(III) compounds are often potent oxidants, we focused on complexes combining palladium with one of the lighter group-13 elements, boron through indium. In the course of these studies, it further turned out that all attempts to prepare boron-containing complexes remained unsuccessful. We attribute this failure to the fact that a boron atom is unable to adopt a coordination number of 5 and form a neutral type **A** complex $[B(X)(catphos)_2Pd]$, whereas a hypothetical cation $[B(catphos)_2Pd]^+$ is presumably too strained and vulnerable to attack of nucleophilic solvents or counter ions to be stable.

Preparation of bimetallic Pd,M(III) complexes with M = Al, Ga, In, was pursued via both the "self-assembly" route (path (i), Scheme 2),[5] and a stepwise process involving reaction of catechol phosphine **2** with $[PdCl_2(cod)]$ (cod = 1,5-cyclo-octadiene) to give chelate complex **D** and further condensation with metal trichlorides or tris-acetylacetonates (reactions (iv), (v) in Scheme 2).[4] The one-step reaction, which had previously provided a high yielding access to Pd,Ga-complex **3a** (Scheme 3, (i)),[5] proved unfeasible for the synthesis of aluminium or indium complexes; spectroscopic studies (^{31}P NMR, ESI-MS) gave no evidence for the formation of defined products. In contrast, reaction of **2** with $[PdCl_2(cod)]$ and $[Ga(acac)_3]$ allowed to access a Pd,Ga-complex under base-free conditions (Scheme 3, (ii)). The product was isolated by direct crystallization from the reaction mixture, and characterisation by NMR data and single-crystal X-ray diffraction (see below) revealed the presence of a solvate complex **3b** which differs from **3a** in the coordination of an additional solvent molecule (DMF) at the gallium centre.

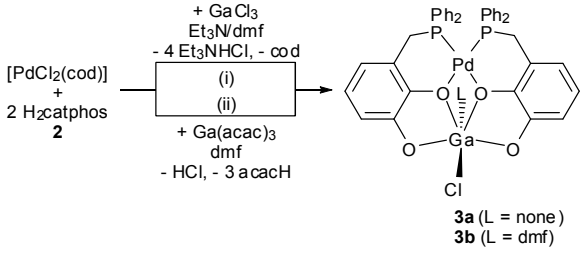

Scheme 3 Synthesis of heterometallic Pd,Ga-complexes from **2** and $GaCl_3$ and $Ga(acac)_3$ (DMF = dimethyl formamide; cod = 1, 5-cyclooctadiene).

As in the case of type **A** complexes with palladium and early transition metals,[4] otherwise inaccessible Pd,Al- and Pd,In-complexes were readily available from the pre-formed Pd-

chelate [Pd(catphosH)$_2$] (**4**, type **D** with M' = Pd in Scheme 2) and metal tris-acetylacetonates [M(acac)$_3$] (M = Al, In) or InCl$_3$, respectively. Reactions of **4** with [Al(acac)$_3$] in polar aprotic solvents were sluggish, but clean transformations were observed in methanol at 50 °C (in order to overcome the low solubility of **4** at ambient temperature); presumably, the protic nature of this solvent and its ability to act as hydrogen bridge donor facilitate the proton transfer steps associated with the displacement of the acac-ligands on Al under concomitant generation of the weak acid acacH. Reaction of equimolar amounts of **4** and [Al(acac)$_3$] under these conditions afforded thus after work-up a moderate yield of Pd,Al-complex **5** (Scheme 4) which was identified by a single-crystal XRD study (see below). Spectroscopic characterisation of the product was rather difficult due to its high tendency to hydrolyse in solution. ESI-MS and NMR data confirmed the presence of the intact complex (see Experimental), but indicated also that extensive protolysis to give **4** along with acacH and unidentified Al-containing species took place. ESI mass spectra allowed further to detect a cation [Pd$_2$(μ-catphos)$_4$Al]H$_2^+$, the presence of which might point to the formation of a trinuclear complex, possibly of type **B** (Scheme 1), in the decomposition process.

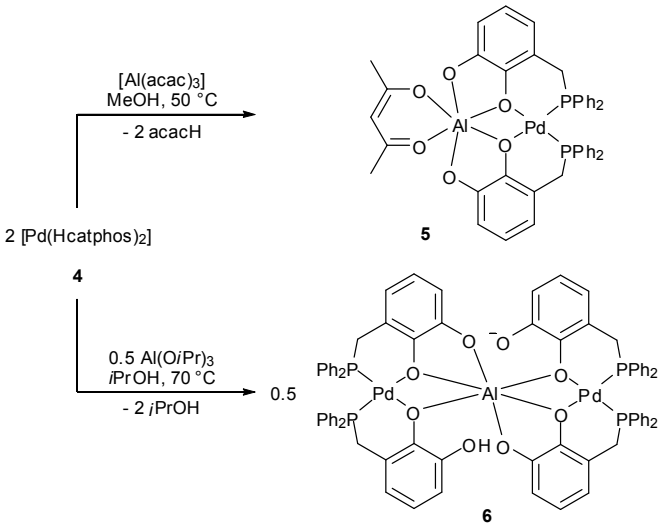

Scheme 4 Synthesis of heterometallic Pd,Al-complexes from **4**.

Since **4** also undergoes condensation with metal alkoxides,[4] we explored its behaviour towards Al(O*i*Pr)$_3$. Reaction of equimolar amounts of reactants in isopropanol at 70 °C gave a crystalline precipitate that was identified as trinuclear type **B** complex **6** (Scheme 4) by solid-state NMR and single-crystal XRD studies. Even if the ESI-MS displayed the ion peak of the protonated complex, NMR data gave no conclusive results. The spectra of fresh solutions displayed broadened signals that prevented a concise structural assignment. Aged solutions showed evidence for hydrolysis.

Reaction of **4** and InCl$_3$ requires no protic solvent but proceeds, by analogy to the formation of gallium complex **3a**, smoothly in a CH$_2$Cl$_2$/Et$_3$N mixture. Work-up afforded a product which was readily identified as tetranuclear complex **7** (Scheme 5) by a single-crystal XRD study. The dominant peak in the (+)-ESI-MS is attributable to a cation [Pd(catphos)$_2$In]$^+$ formed by loss of chloride from the basic binuclear unit of the complex, but the spectrum also contains a low intensity peak at higher m/e ratio that is attributable to a trinuclear Pd$_2$In species. The deliberate synthesis of a complex with this structural motif was feasible by reacting equimolar amounts of **4** and [In(acac)$_3$] at 50 °C in methanol. The product was isolated in excellent yield (86% with respect to **4**) after partial evaporation of the solvent and crystallization. Even if the material was unsuitable for single-crystal X-ray diffraction, its identity as neutral complex **8** was established by peaks of pseudo-molecular ions [In(catphos)$_4$Pd$_2$]H$_2^+$ and [In(catphos)$_4$Pd$_2$]NaH$^+$ in the (+)-ESI-MS, and confirmed by solution NMR studies (see below).

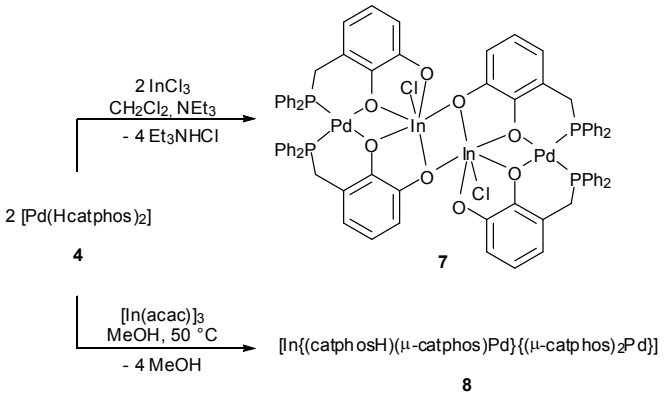

Scheme 5 Synthesis of heterometallic Pd,In-complexes from **4**.

Crystallographic studies

The molecular structures of **3b**, **5** – **7** and selected structural parameters are displayed in Figures 1 – 4. All four complexes share a distorted square planar coordination at palladium. The coordination number at the group-13 element is always six, but individual complexes show a remarkable variety in coordination geometries and bonding modes of the bridging catechol phosphine units, as well as a large conformational flexibility of the four-membered PdMO$_2$-rings that form the core of the heterometallic assembly.

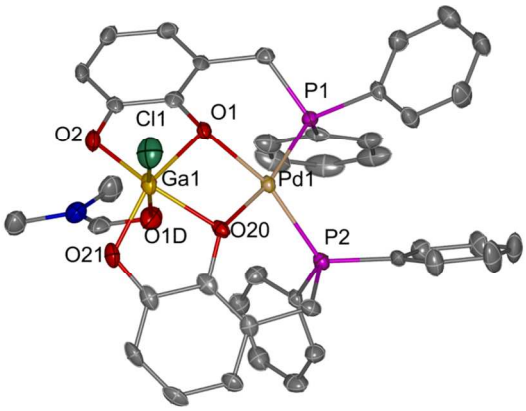

Figure 1 ORTEP-style representation of the molecular structure of **3b** in the crystal. Thermal ellipsoids are drawn at 50% probability level; hydrogen atoms

are omitted for clarity. Selected distances (in Å) and angles (in °): Pd1-P1 2.247(2), Pd1-P2 2.248(2), Pd1-O1 2.060(3), Pd1-O20 2.056(3), Ga1-O1 2.025(4), Ga1-O2 1.872(4), Ga1-O20 1.998(4), Ga1-O21 1.891(4), Ga1-Cl1 2.195(2), Ga1-O1D 2.823(4), O20-Pd1-O1 74.8(1), P1-Pd1-P2 102.2(1).

The square pyramidal layout of the chlorine and catecholato-oxygen atoms around the gallium centre and the bowl-like arrangement of the catecholate ring planes in **3b** (Figure 1) resemble closely the characteristic structural features of **3a**.[5] The oxygen atom of the extra DMF ligand occupies a *trans*-position with respect to the chloride, but the Ga1–O1D separation (2.823(4) Å) is noticeably longer than the other Ga–O distances (1.872(4) – 2.025(4) Å) and suggests to describe the coordination number at gallium as 5+1 rather than 6. In total, the geometrical distortions induced by the additional ligand are – apart from the different orientation of phenyl rings) relatively small, which is also illustrated in the similarity of O–Pd–O and P–Pd–P bite angles in **3a** [5] (O–P–O 74.3(1)°, P–Pd–P 101.8(1)°) and **3b** (O–P–O 74.8(1)°, P–Pd–P 102.2(1)°).

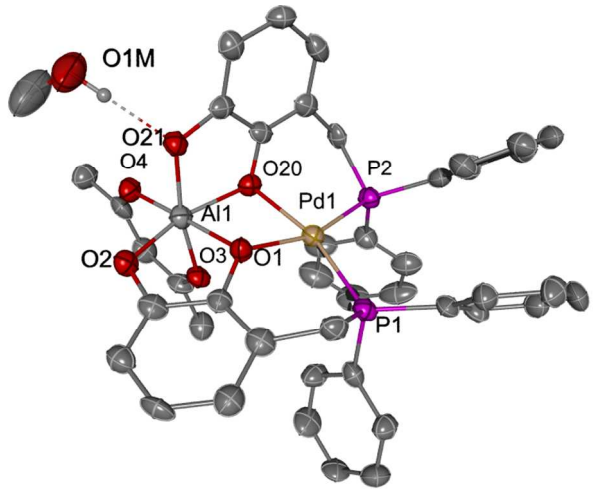

Figure 2 ORTEP-style representation of the molecular structure of **5** in the crystal. Thermal ellipsoids are drawn at 50% probability level; hydrogen atoms in CH bonds and the second solvent molecule in the structure are omitted for clarity. Selected distances (in Å) and angles (in °): Pd1-P1 2.224(2), Pd1-P2 2.230(2), Pd1-O1 2.017(5), Pd1-O20 2.087(5), Al1-O1 1.920(5), Al1-O2 1.834(5), Al1-O20 1.964(5), Al1-O21 1.862(5), Al1-O3 1.920(5), Al1-O4 1.851(6), O21···O1M 2.652(9), O1-Pd1-O20 75.1(2), P1-Pd1-P2 106.1(1).

The molecular structure of **5** (Figure 2) differs from that of **3b** mainly in the fact that the oxygen atoms of the three bidentate ligands in the Al-tris-chelate unit occupy mutual *cis*-positions, and that the two catecholate units have therefore markedly different orientations: one μ-bridging oxygen atms (O1) retains a nearly trigonal planar coordination sphere (sum of bond angles 347(1)°), and the adjacent benzene ring remains nearly parallel to the central AlO_2Pd ring plane; the coordination at the other μ-bridging oxygen atom (O20) is pyramidal (sum of bond angles 311(1)°), and the flanking benzene ring exhibits a strong tilt with respect to the AlO_2Pd ring. The Al–O distances in **5** (1.834(5) – 1.964(5) Å) are generally shorter than the Ga–O distances in **3b** (1.872(4) – 2.025(4) Å), in line with the smaller effective ion radius for Al^{3+} (0.535 Å, vs. 0.620 Å for Ga^{3+} [9]). As had been previously noted,[5] decreasing the size of the template increases the bite angle of the bis-phosphine unit at palladium (P–Pd–P 106.1(1) vs. 102.2(1) in **3b**). Attachment of a hydrogen bridge donor to one of the terminal catecholato-oxygen atoms has precedence in an analogous Ti,Pd-complex [4] and induces a slight lengthening of the Al–O bond (1.862(5) Å for O21-Al1 vs. 1.834(5) for O2-Al1).

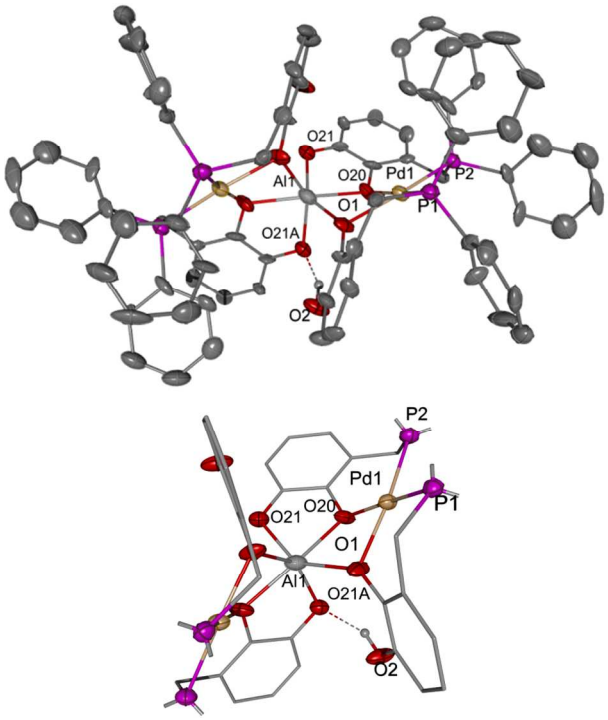

Figure 3 ORTEP-style representation of the molecular structure of **6** in the crystal (top) and reduced representation without phenyl rings (bottom). Thermal ellipsoids are drawn at 50% probability level; hydrogen atoms in CH bonds are omitted for clarity. Only one of two split positions for the hydrogen atom on O2 is displayed. Selected distances (in Å) and angles (in °): Pd1-P1 2.214(3), Pd1-P2 2.220(3), Pd1-O1 2.052(5), Pd1-O20 2.005(6), Al1-O1 2.145(8), Al1-O20 2.094(7), Al1-O21 2.021(7), O1-Pd1-O20 76.3(3), P1-Pd1-P2 97.2(1).

Complex **6** (Figure 3) has crystallographic C_2-symmetry. The aluminium atom binds to six of the eight oxygen atoms of two chelating {(catphos)$_2$Pd} "pseudo-ligands" in a highly distorted coordination environment that is intermediate between regular octahedral and trigonal prismatic. Analysis of the distortion with the "twist angle" model reveals a twist of some 22° between the basal faces of the prism, which corresponds to a 37% distortion towards octahedral.[10] The three oxygen donor atoms in each unit are found at larger distances (Al–O 2.021(7) – 2.145(8) Å) than in **5**. The distance to the remaining oxygen atom (Al–O2 3.626(9) Å) is close to the sum of van-der-Waals radii (3.75 Å [11]). Electroneutrality requires the presence of one further proton which is split between two sites close to the non-bound oxygen atoms. The O2···O21A distance (2.673(10) Å) and the large O2–H···O21A angle (153°) suggest that this proton is involved in a hydrogen bond which connects the chelating pseudo-ligands. The coordination at the μ-bridging O1 atom of the monodentate catechol(ate) is planar (sum of bond angles 360°) whereas the O20 atom in the bidentate catecholate is slightly pyramidal (sum of bond angles 340°).

The O20–Pd1–O1 angle (76.3(3)°) is slightly larger and the P1–Pd1–P2 bite angle (97.2(1)°) distinctly smaller than in **5**. Both effects together render the deviation from regular square planar coordination at palladium less pronounced; a comparison of Al–O distances in **5** and **6** suggests, however, that this geometric relaxation is offset by destabilisation of the aluminium coordination sphere.

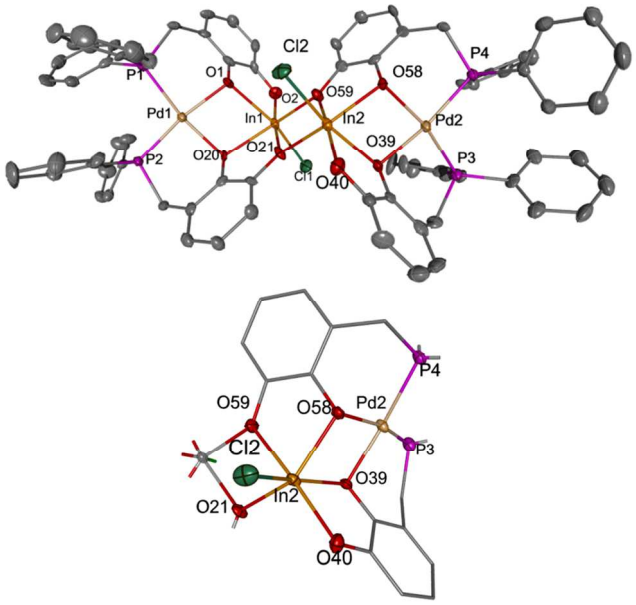

Figure 4 ORTEP-style representation of the molecular structure of **7** in the crystal (top) and reduced representation showing the metal coordination environment in one half of the molecule (bottom). Thermal ellipsoids are drawn at 50% probability level; hydrogen atoms are omitted for clarity. Selected distances (in Å) and angles (in °): In1-O1 2.271(5), In1-O2 2.097(5), Pd1-P1 2.250(2), Pd1-P2 2.254(2), Pd1-O1 2.080(4), Pd1-O20 2.082(5), In1-O20 2.231(4), In1-O21 2.191(5), In1-O59 2.162(4), In1-Cl1 2.413(2), Pd2-P3 2.257(2), Pd2-P4 2.263(2), Pd2-O39 2.078(4), Pd2-O58 2.082(5), In2-O21 2.153(4), In2-O39 2.267(5), In2-O40 2.098(5), In2-O58 2.218(4), In2-O59 2.201(5), In2-Cl2 2.414(2), O1-Pd1-O20 80.6(2), P1-Pd1-P2 100.0(1), O39-Pd2-O58 81.2(2), P3-Pd2-P4 101.8(1).

Tetranuclear complex **7** (Figure 4) is best described as the product of mutual donor/acceptor-interaction of two binuclear complexes [In(Cl)(μ-catphos)$_2$Pd]. The pairing creates a new rhombic In_2O_2 ring in which bridging In1–O59 and In2–O21 distances (2.153(4) – 2.162(4) Å) are shorter than internal In1–O21 and In2–O59 distances (2.191(5) – 2.201(5) Å) between atoms in the same fragment. The dimerization is presumably induced by the coordinative unsaturation of the large group-13 template (ionic radius of In^{3+} 0.80 Å [9]) in an isolated [In(Cl)(catphos)$_2$Pd] fragment. Even if this aggregation has precedence in a bismuth complex [Bi(Cl)(catphos)$_2$Pd] (**9**),[5] both species show some notable structural differences: the subunits of **9** are linked via chloride bridges, whereas those of **7** are held together by μ-bridging oxygen donors and the chlorides act as terminal ligands; furthermore, the *cisoid* orientation of the catecholate ligands in **9** imposes effective local mirror symmetry around the BiO_2Pd rings, whereas **7** exhibits a *transoid* alignment with effective local C_2-symmetry for each In(catphos)$_2$Pd unit.

Comparing the local environment of the palladium atom in **3b**, **5** – **7** confirms previous evidence [5] that variation of the M(L)$_n$ template in a complex [M(L)$_n$(catphos)$_2$Pd] allows to tune P–Pd–P bite angles over a remarkably wide range (from 97° in **5** to 106° in **6**). The structural consequences of a formal exchange of templates are, however, not foreseeable, and the finding that both the largest and smallest bite angles occur in aluminium-containing complexes indicate that the variations cannot be explained by simple rules. The conjecture that larger templates decrease the separation between the phosphorus atoms and enforce thus smaller bite angles [5] holds thus at best for a very limited subset of compounds and cannot be generalised.

Solution NMR studies

Apart from helping in the constitutional assignment of complexes **3b**, **5** – **8**, solution NMR studies yielded information on conformational dynamics and ligand exchange processes which provide deeper insight into the flexibility and stability of the multimetallic frameworks.

The ^{1}H NMR spectra of Al(III) complexes **5**, **6** contain broad signals that cannot be assigned to individual species but suggest that the complexes have experienced a structural collapse or underwent partial hydrolysis in solution. This interpretation was confirmed by detection of the signal of **4** as major constituent in ^{31}P NMR spectra of aged solutions of both complexes. Likewise, the ^{27}Al chemical shifts of **6** in solution (77 ppm) and in the solid state (5 ppm) display a large discrepancy which is incompatible with the presence of the same molecular structure in both phases; the solution shift is rather indicative of an acetylacetonato- or catecholato- complex with five-coordinate aluminium,[12] or a dynamically exchanging mixture of species with different metal coordination numbers.

In combination with ESI-MS data, these findings led us to conclude that the binuclear complexes **5**, **6** exhibit limited stability in solution and tend to disassemble into different species. The formation of substantial amounts of palladium complex **4** suggests cleavage of aluminium-catecholate-bonds as major fragmentation pathway. In view of the abundance of known Al(III) catecholates,[13] the instability of **5**, **6** is presumably not caused by the incompatibility of metal and bidentate catecholate ligands, but by a mismatch between the preorganisation of the two catechol units on the Pd(II) template of **4** and the steric requirements of the metal centre – the molecular structure of **4** is apparently too rigid to arrange the catecholate units for optimum binding of the small Al(III) ion.

The ^{1}H and ^{31}P NMR spectra of the gallium complexes **3a**,**b** display defined signals which do not change with time. The benzylic protons in **3b** give rise to two separate doublets rather than a single broad signal as in **3a**,[5] which implies a slower inversion rate of the square-pyramidal ClO_5-array. This behaviour is readily accounted for if one assumes that the DMF ligand in **3b** is not lost in solution, and dynamic isomerization at the six-coordinate gallium occurs less easily than at the five-coordinate metal centre in **3a**. The persistence of **3a**,**b** in solution suggests that these complexes are thermodynamically stable, which is also in accord with the observation that their

formation via spontaneous condensation of ligand **2** with appropriate metal salts is highly specific and does not yield detectable amounts of side-products.

The ^{1}H and ^{31}P NMR spectra of indium complex **7** reveal severely broadened resonances which sharpen, however, at low temperature (-70 °C) to produce defined signals with a similar pattern as **3a**,**b**. The room temperature lineshape changes upon prolonged storage of the solutions eventually into a different set of broadened signals which appear at comparable chemical shifts as the resonances of **8** (see below). Similar changes were also observable when residual water was present in the samples. Whereas the initial (reversible) temperature dependent signal broadening is presumably associated with conformational dynamics (e. g. inversion of the non-planar chelate rings at the palladium atom) and possible dissociation equilibria involving separation of the molecular subunits of **7**, the long term changes suggest that structural reorganisation and concomitant formation of a new species take place.

Complex **8** is peculiar as its ^{1}H and ^{31}P NMR spectra exhibit resonances of four distinguishable catechol phosphine ligands. The pairwise coupling of the ^{31}P NMR signals to yield two AB-patterns indicates that the ligands form two Pd(catphos)$_2$ units with *cis*-coordinated phosphine donors. An additional ^{1}H NMR signal at low field reveals a single acidic proton which is presumably involved in an intramolecular hydrogen bond. In connection with the ESI-MS data, these findings support the presence of a complex containing a central In(III) ion ligated by a mono-anionic {(catphosH)(catphos)$_2$Pd}$^{-}$ and a dianionic {(catphos)$_2$Pd}$^{2-}$ unit (Scheme 5). Two-dimensional ^{1}H and ^{31}P EXSY spectra disclose, however, that the molecular structure of **8** is not static, but that reversible exchange processes induce dynamic averaging of the unlike ligand environments. Analysis of the changes in cross-peak patterns with temperature and mixing time reveal that full equalisation is accomplished in several stages which exhibit different activation energies. A consistent mechanistic picture can be developed if **8** is assigned a similar structure as aluminium complex **6**. The transformation with the lowest energy barrier involves pairwise exchange between catechol phosphines in different {(catphos)$_2$Pd} units but does not mix signals of ligands at the same palladium centre (Figure 5a), and can be associated with a transfer of the hydroxylic proton along the H-bridge to a metal-bound oxygen atom in the other {(catphos)$_2$Pd} unit, and subsequent rearrangement of the catecholates (Scheme 6, reaction (i)).

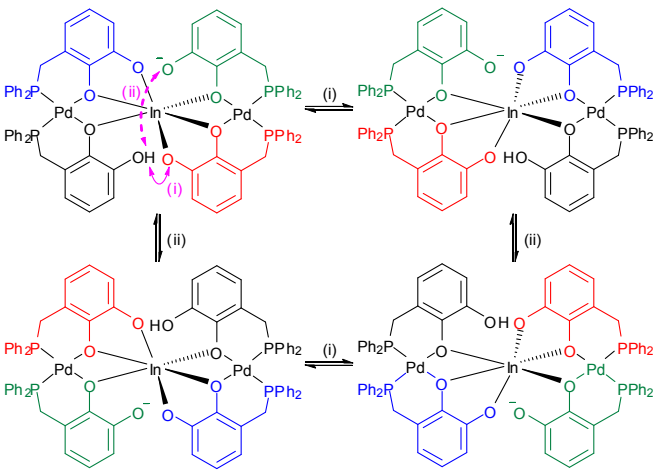

Scheme 6 Schematic representation of the proposed mechanism for dynamic averaging between distinguishable catechol phosphine ligands in **8**.

At the next stage, averaging between the ligands in the same {(catphos)$_2$Pd} unit is observed (Figure 5b), which we explain as a result of a transfer of the hydroxylic proton to the remote free catecholate site (Scheme 6, reaction (ii)). Finally, exchange between inequivalent benzylic protons in each ligand indicates the onset of conformational inversion of the non-planar, six-membered Pd-centred chelate rings.

The conservation of the multiplet structure in the ^{31}P NMR spectra suggests that all exchange processes are intramolecular. It must be admitted that the available spectroscopic data do not allow secure assignment of the coordination geometry around the central indium atom. However, the mechanistic explanation remains valid even if the metal centre extends its coordination by binding of one or both of the "free" catecholate oxygen donors, and may thus serve as a general model which can also explain the rapid dynamic averaging of ligand environments in other protonated catechol phosphine complexes.[6]

The finding that even extended storage of solutions of **8** does not result in perceptible disintegration attests this complex a higher stability compared to binuclear **7** (which is also fully in accord with the observed formation of **8** during degradation of **7**). This trend is in contrast to the case of the gallium complexes **3a**,**b**, which give no evidence for the formation of an analogous trinuclear assembly, and highlights once more the importance of template size as a critical factor for the stabilisation of multimetallic aggregates with bridging catechol phosphines.

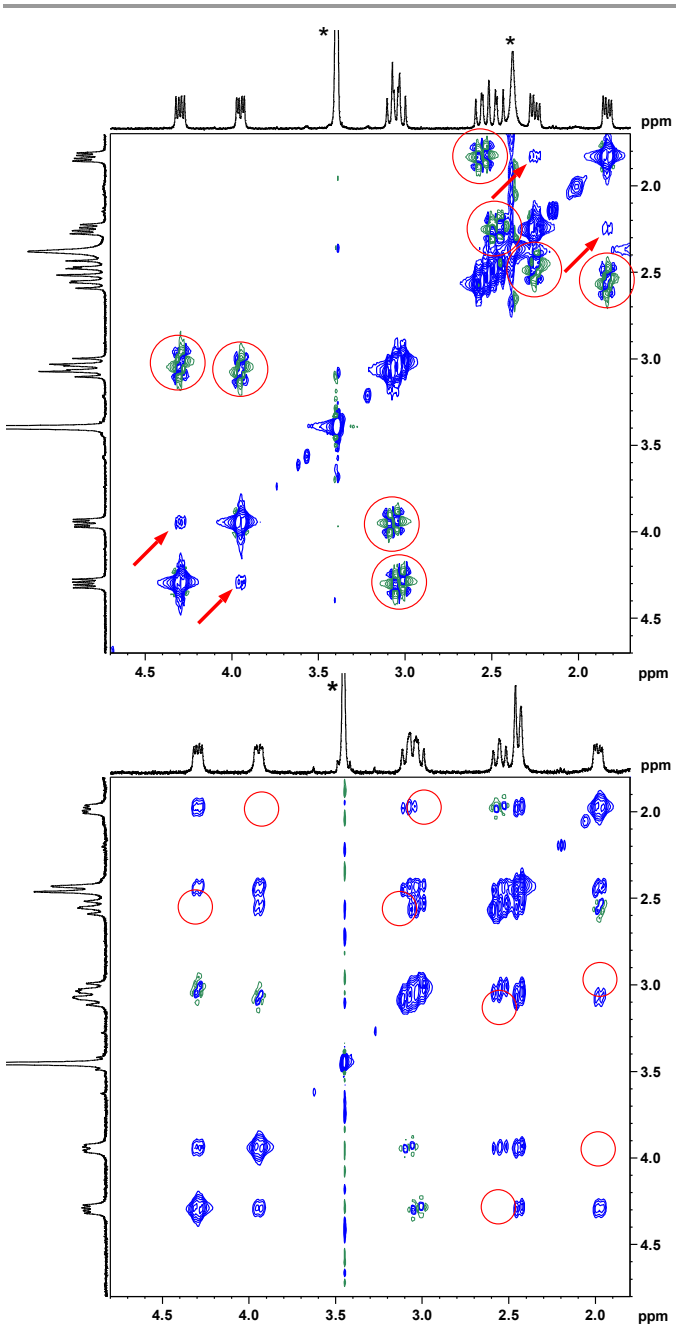

Figure 5 Expansion of the benzylic region of ^{1}H EXSY spectra of **8** (resonances marked with an asterisk are due to MeOH). Top: spectrum recorded at 253 K with 125 ms mixing time. Red circles indicate cross-peaks arising from intramolecular NOE and *J*-coupling breakthrough; red arrows denote peaks due to exchange between different catphos ligands. Bottom: spectrum recorded at 303 K with 50 ms mixing time. Red circles denote missing cross-peaks which would indicate exchange between anisochronous benzylic protons in the same ligand; these peaks become visible when longer mixing times (> 200 ms) are employed (see supporting information).

Conclusions

The ability of catechol phosphine **2** to support di- and trinuclear heterometallic complexes containing palladium and the group-13 elements aluminium, gallium, and indium was demonstrated. The target complexes were either accessed via spontaneous reactions between the ligand and two simple metal salts, or by condensation of pre-formed palladium chelate [Pd(catphosH)$_2$] with group-13 element acetylacetonates or alkoxides. Crystallographic and solution NMR data indicate that the match between the size of the group-13 ion and the preorganisation of the donor centres in the rigid {Pd(catphos)$_2$} unit has a critical effect on complex stabilities. Heterometallic assemblies with Al(III) are unstable in solution since this cation is obviously too small for the Pd-centred pseudo-chelate ligand. Complexes [GaCl(L)(catphos)$_2$Pd] built around a larger Ga(III) centre that is either pentacoordinate (L = –) or accommodates a secondary ligand (L = DMF) seem to provide a perfect match, which is reflected in both high formation tendency and increased stability in solution. The still larger In(III) cation supports formation of a complex [InCl(catphos)$_2$Pd], which dimerises in the solid state under formation of intermolecular In–O bonds but rearranges in solution to give rise to a trinuclear assembly of composition [In{(catphos)$_2$Pd}$_2$]H. The superior stability of this species is underlined by its formation as main product in the reaction of equimolar amounts of In(acac)$_3$ and [Pd(catphosH)$_2$], and confirms the hypothesis [5,6] that the tendency of large metal cations to adopt higher coordination numbers provides a strong driving force for formation of the M{(catphos)$_2$Pd}$_2$ binding motif. NMR studies allowed to follow the dynamic averaging of the four different catechol phosphine environments in the trinuclear framework, and to propose a mechanism for this process which involves a sequence of discernible proton transfer and ligand rearrangement steps, and may serve as a model for the explanation of analogous dynamics in related complexes.

Experimental

Materials and Methods

All manipulations were carried out under dry argon using standard Schlenk techniques. Solvents were purified by standard procedures. NMR spectra: Bruker Avance 250 (^{1}H: 250.1 MHz, ^{31}P: 101.2 MHz) or Avance 400 (^{1}H: 400.1 MHz, ^{27}Al: 104.0 MHz, ^{31}P: 162.9 MHz) at 30 °C. Chemical shifts were referenced to ext. TMS (^{1}H), 1.1 M Al(NO$_3$)$_3$ (^{27}Al; Ξ = 26.056859 MHz), or 85 % H$_3$PO$_4$ (^{31}P; Ξ = 40.480742 MHz). Coupling constants are given as absolute values. Elemental analyses: Perkin-Elmer 2400 CHSN/O Analyser. (+)-ESI mass spectra: Bruker Daltonics MicroTOF Q instrument. MeOH was used as solvent unless specified otherwise. Melting Points were determined with a Büchi B-545 melting point apparatus in sealed capillaries.

Complex **3b**: [Ga(acac)$_3$] (104 mg, 0.32 mmol), [PdCl$_2$(cod)] (102 mg 0.32 mmol) and Et$_3$N (0.2 ml, 1.44 mmol) were added to a solution of **2** (200 mg, 0.65 mmol) in 10 ml of DMF. The mixture was stirred for 3 h and was then evaporated to dryness. Recrystallization of the red brown residue from DMF/Et$_2$O (1:1) yielded 162 mg (0.19 mmol, 60 %) of **3b** of m. p. 215 – 216 °C. – ^{1}H NMR (CDCl$_3$): δ = 7.62 - 7.25 (m, 8 H, *o*-Ph), 7.09 - 6.87 (m, 12 H, *m-/p*-Ph), 6.61 (d, $^{3}J_{HH}$ = 7.8 Hz, 2 H,

C_6H_3), 6.44 (t, $^3J_{HH}$ = 7.8 Hz, 2 H, C_6H_3), 6.02 (d, $^3J_{HH}$ = 7.8 Hz, 2 H, C_6H_3), 3.95 (dd, $^2J_{HH}$ = 17.0 Hz, $^3J_{PH}$ = 12.2 Hz, 2 H, CH_2), 3.35 (dd, $^2J_{HH}$ = 17.0 Hz, $^2J_{PH}$ = 11.9 Hz, 2 H, CH_2). – $^{31}P\{^1H\}$ NMR ($CDCl_3$): δ = 64.1 (s). – (+)-ESI-MS: *m/e* = 786.99 $[M\text{-}Cl]^+$. – (–)-ESI-MS: *m/e* = 840.97 $[M+OH]^-$. – Anal. for $C_{38}H_{30}ClGaO_4P_2Pd \cdot DMF$ (897.28 g mol^{-1}): calcd. C 54.88, H 4.16, N 1.56%; found C 53.88, H 4.56, N 1.12 %.

Complex 5: $[Al(acac)_3]$ (54 mg, 0.17 mmol) was added to a suspension of **4** (120 mg, 0.17 mmol) in 15 ml of MeOH. The mixture was heated to 50 °C and stirred for 3 h until all solids had dissolved. The red solution formed was then concentrated to approx. one third of its original volume, allowed to cool to r.t., and stored for 48 h at 4 °C. The red crystalline precipitate formed was collected by filtration and dried under reduced pressure. Yield: 43 mg (51 µmol, 31 %), m. p. 108 – 110 °C. – ^1H NMR (CD_2Cl_2): δ = 7.63 – 7.52 (br m, 2 H, Ph), 7.50 – 6.78 (m, 18 H, Ph), 6.75 – 6.54 (m, 4 H, C_6H_3), 6.20 (m, 2 H, C_6H_3), 5.51 (s, 1 H, CH), 3.39 (br, 4 H, CH_2), 1.93 (br s, 6 H, CH_3). – $^{31}P\{^1H\}$ NMR (CD_2Cl_2): δ = 79.4 (s). – (+)-ESI-MS: *m/e* = 745.05 $[M\text{-}acac]^+$, 845.10 $[M+H]^+$. – Anal. for $C_{43}H_{37}AlO_6P_2Pd \cdot CH_3OH$ (877.15 g mol^{-1}): calcd. C 60.25, H 4.71%; found C 60.58, H 4.66 %.

Complex 6: $Al(O\textit{i}Pr)_3$ (34 mg 0.17 mmol) was added to a suspension of **4** (120 mg, 0.17 mmol) in 10 ml *i*PrOH. The mixture was heated to 70 °C and stirred for 3 h until all solids had dissolved. The red solution formed was then concentrated to approx. one third of its original volume, and allowed to cool to r.t. A bright red solid precipitated within 24 h. The supernatant solution, which had become almost colourless, was discarded, and the crystalline residue dried under reduced pressure. Single-crystals suitable for a XRD study were obtained by recrystallization from CH_2Cl_2 at -20 °C. Yield 85 mg (58 µmol, 35 %), m. p. 156 – 157 °C. – ^1H NMR (CD_2Cl_2): δ = 7.38 (s br, 1 H, OH), 7.37 - 7.31 (m, 8 H, Ph), 7.28 - 7.21 (m, 16 H, Ph), 7.20 - 7.13 (m, 16 H, Ph), 6.73 (d, $^3J_{HH}$ = 7.6 Hz, 4 H, C_6H_3), 6.29 (t, $^3J_{HH}$ = 7.6 Hz, 4 H, C_6H_3), 6.18 (d, $^3J_{HH}$ = 7.3 Hz, 4 H, C_6H_3), 3.44 – 3.39 (m, 8 H, CH_2). – $^{31}P\{^1H\}$ NMR (CD_2Cl_2): δ = 61.3 (s). – ^{27}Al NMR (CD_2Cl_2): δ = 77.0 (s). – $^{31}P\{^1H\}$ CP-MAS NMR: δ = 53.0, 49.0; $^2J_{PP}$ = 31 Hz (from 2D J-resolved). – $^{27}Al\{^1H\}$ CP-MAS NMR: δ = 5.0. – (+)-ESI-MS: m/e = 1465.13 $[M+H]^+$. The presence of varying amounts of residual solvent in bulk samples prevented to obtain a satisfactory elemental analysis.

Complex 7: $InCl_3$ (24 mg, 0.11 mmol) and Et_3N (0.05 ml, 0.36 mmol) were added to a solution of **4** (80 mg, 0.11 mmol) in 12 ml of CH_2Cl_2. The mixture was stirred overnight and then evaporated to dryness. Recrystallization of the red brown residue from acetone produced 45 mg (51 µmol, 46 %) of **7**, m. p. >250 °C (dec). – ^1H NMR (acetone-d_6, 303 K): 7.6 – 7.0 (br, 40 H, Ph), 7.0 – 5.6 (br, 12 H, C_6H_3, 3.3 – 3.1 (br, 8 H, CH_2). – $^{31}P\{^1H\}$ NMR (acetone-d_6, 303 K): δ = 71.2 (br d, $^2J_{PP}$ = 42 Hz), 67.9 (br d, $^2J_{PP}$ = 42 Hz), 55.2 (br), 50.8 (br). – ^1H NMR (CD_2Cl_2, 203 K): 7.32 (br m, 12 H, Ph), 7.22 – 7.12 (br m, 12 H, Ph), 6.88 (br m, 16 H, Ph), 6.58 (d, $^3J_{HH}$ = 8 Hz, 4 H, C_6H_3), 6.29 (t, $^3J_{HH}$ = 8 Hz, 4 H, C_6H_3), 5.62 (d, $^3J_{HH}$ = 8 Hz, 4 H, C_6H_3), 3.79 (br d, $^2J_{HH}$ = 12.4 Hz, 4 H, CH_2), 2.98 (br m, 4 H, CH_2). – $^{31}P\{^1H\}$ NMR (CD_2Cl_2, 203 K): δ = 74.8 (s). – (+)-ESI-MS: *m/e* = 832.98 $[In(L)_2Pd]^+$. – Anal. for $C_{76}H_{60}O_8P_4Pd_2In_2Cl_2 \cdot 4$ acetone (1970.91): calcd. C 53.63, H 4.30%; found C 54.06, H 4.02%.

Complex 8: $[In(acac)_3]$ (103 mg, 0.25 mmol) were added to a suspension of **4** (180 mg, 0.25 mmol) in 20 ml of MeOH. The mixture was heated to 50 °C and stirred for 3 h until all solids had dissolved. The red solution formed was then concentrated to approx. one third of its original volume, and allowed to cool to r.t. Et_2O was added until the clear solution became turbid. The resulting mixture was stored for 48 h at 4 °C to produce a dark red, microcrystalline solid which was collected by filtration and dried under reduced pressure to yield 168 mg (0.11 mmol, 86 % with respect to **4**) of **8**, m. p. 136 – 137 °C. – ^1H NMR (400 MHz, 303 K, CD_2Cl_2): δ = 11.32 (s, 1 H, OH), 8.08 (m, 2 H, Ph), 7.50 (m, 1 H, Ph), 7.45 (m, 2 H, Ph), 7.41 – 7.17 (m, 18 H, Ph), 7.17 – 6.94 (m, 16 H, Ph + 1 H, C_6H_3), 6.94 – 6.84 (m, 1 H, Ph + 2 H, C_6H_3), 6.74 (d, $^3J_{HH}$ = 7.4 Hz, 1 H, C_6H_3), 6.55 (d, $^3J_{HH}$ = 7.4 Hz, 2 H, C_6H_3), 6.40 (t, $^3J_{HH}$ = 7.6 Hz, 2 H, C_6H_3), 6.21 (t, $^3J_{HH}$ = 7.5 Hz, 1 H, C_6H_3), 5.90 (d, $^3J_{HH}$ = 7.7 Hz, 1H, C_6H_3), 5.85 (d, $^3J_{HH}$ = 7.9 Hz, 1 H, C_6H_3), 5.70 (d, $^3J_{HH}$ = 7.2 Hz, 1 H, C_6H_3), 5.61 (d, $^3J_{HH}$ = 7.2 Hz, 1 H, C_6H_3), 4.30 (dd, $^2J_{PH}$ = 6.2 Hz, $^2J_{HH}$ = 12.4 Hz, 1 H, CH_2), 3.94 (dd, $^2J_{PH}$ = 4.3 Hz, $^2J_{HH}$ = 12.0 Hz, 1 H, CH_2), 3.08 (dd, $^2J_{PH}$ = 16.8 Hz, $^2J_{HH}$ = 12.4 Hz, 1 H, CH_2), 3.03 (dd, $^2J_{PH}$ = 18 Hz, $^2J_{HH}$ = 14 Hz, 1 H, CH_2), 2.55 (t, $^2J_{PH}$ = $^2J_{HH}$ = 14 Hz, 1 H, CH_2), 2.44 (d, $^2J_{HH}$ = 13.0 Hz, 2 H, CH_2), 1.98 (d, $^2J_{PH}$ = 5.6 Hz, $^2J_{HH}$ = 12.3 Hz, 1 H, CH_2). – $^{31}P\{^1H\}$ NMR (161.9 MHz, 303 K, CD_2Cl_2): δ = 71.6 (d, $^2J_{PP}$ = 49 Hz), 68.2 (d, $^2J_{PP}$ = 49 Hz), 54.9 (dd, $^2J_{PP}$ = 33 Hz), 48.9 (dd, $^2J_{PP}$ = 33 Hz). ^1H NMR (400 MHz, 253 K, CD_2Cl_2): δ = 11.35 (s, 1 H, OH), 8.03 (m, 2 H, Ph), 7.53 (m, 1 H, Ph), 7.47 (m, 2 H, Ph), 7.41 - 7.17 (m, 17 H, Ph), 7.14 - 6.93 (m, 14 H, Ph + 1 H, C_6H_3), 6.90 - 6.77 (m, 2 H, Ph + 3 H, C_6H_3), 6.55 (d, $^3J_{HH}$ = 7.8 Hz, 1 H, C_6H_3), 6.37 (t, $^3J_{HH}$ = 7.6 Hz, 1 H, C_6H_3), 6.36 (t, $^3J_{HH}$ = 7.6 Hz, 1 H, C_6H_3), 6.25 (t, $^3J_{HH}$ = 7.6 Hz, 1 H, C_6H_3), 6.22 (t, $^3J_{HH}$ = 7.6 Hz, 1 H, C_6H_3), 5.97 (d, $^3J_{HH}$ = 7.4 Hz, 1 H, C_6H_3), 5.82 (d, $^3J_{HH}$ = 7.2 Hz, 1 H, C_6H_3), 5.70 (d, $^3J_{HH}$ = 7.2 Hz, 1 H, C_6H_3), 5.64 (d, $^3J_{HH}$ = 7.4 Hz, 1 H, C_6H_3), 4.30 (dd, $^2J_{HH}$ = 13.0 Hz, $^2J_{PH}$ = 6.8 Hz, 1 H, CH_2), 3.95 (dd, $^2J_{PH}$ = 5.2 Hz, $^2J_{HH}$ = 12.0 Hz, 1 H, CH_2), 3.07 (t, $^2J_{PH}$ = $^2J_{HH}$ = 12.3 Hz, 1 H, CH_2), 3.03 (t, $^2J_{PH}$ = $^2J_{HH}$ = 13.3 Hz, 1 H, CH_2), 2.56 (dd, $^2J_{PH}$ = 16.4 Hz, $^2J_{HH}$ = 13.2 Hz, 1 H, CH_2), 2.48 (dd, $^2J_{PH}$ = 18.0 Hz, $^2J_{PH}$ = 14.3 Hz, 1 H, CH_2), 2.50 (t, $^2J_{PH}$ = 18.0 Hz, 1 H, CH_2), 2.25 (dd, $^2J_{PH}$ = 7.0 Hz, $^2J_{HH}$ = 14.0 Hz, 1 H, CH_2), 1.83 (dd, $^3J_{HH}$ = 6.0 Hz, $^2J_{PH}$ = 12.6 Hz, 1 H, CH_2). – $^{31}P\{^1H\}$ NMR (161.9 MHz, 253 K, CD_2Cl_2): δ = 71.3 (d, $^2J_{PP}$ = 47 Hz), 68.5 (d, $^2J_{PP}$ = 47 Hz), 54.2 (d, $^2J_{PP}$ = 32 Hz), 48.2 (d, $^2J_{PP}$ = 32 Hz). Anal. for $C_{76}H_{61}InO_8P_2Pd_2 \cdot 4$ MeOH (1682.04): calcd. C 57.12, H 4.61%, found C 56.91, H 4.47%. – (+)-ESI-MS (MeOH): *m/e* = 832.98 $[In(L)_2Pd]^+$, 1555.06$[M+H]^+$, 1577.04 $[M+Na]^+$.

X-ray diffraction studies

Diffraction data were collected at 123(2) K using a Bruker-Nonius Kappa-CCD diffractometer with Mo-K_α radiation (λ = 0.71073 Å). A combination of ω and Φ scans was carried out to obtain at least a unique data set. Direct methods (SHELXS-97 [14]) were used for structure solution (dual space methods for **5**, using SHELXD [14]). Refinement was carried out using SHELXL-97 [14] (full-matrix least-squares on F^2). Non-hydrogen atoms were refined anisotropically and hydrogen atoms with a riding model (H(O) free). Semi-empirical absorption corrections were applied.

One chloroform molecule in **3a** is disordered. Three acetone molecules in **7** are disordered, and some phenyl groups in **6** and **7** show high displacement parameters, indicating a possible disorder which could not be resolved due to limited data quality. Four highly disordered solvent molecules (CH_2Cl_2) in the crystal structure of **6** were removed using the SQUEEZE routine in the program Platon.[15] Details of the crystal structure determinations are listed in Table 1 and in the cif-files (see ESI). Crystallographic data (excluding structure factors) have been deposited with the Cambridge Crystallographic Data Centre as supplementary publication no. CCDC-990576 (**3a**), CCDC-990577 (**3b**), CCDC-990578 (**5**), CCDC-990579 (**6**), and CCDC-990580 (**7**). Copies of the data can be obtained free of charge on application to: The Director, CCDC, 12 Union Road, GB-Cambridge CB2 1EZ (fax int. +1223/336033; E-mail: deposit@ccdc.cam-ak.uk.

Table 1 Summary of crystallographic data for **3a**, **3b**, **5** – **7**

	3b	**5**	**6** [a)]	**7**
Formula	$C_{41}H_{37}ClGaNO_5P_2Pd$	$C_{43}H_{37}AlO_6P_2Pd$ - 2 MeOH	$C_{76}H_{61}AlO_8P_4Pd_2$ - 2 CH_2Cl_2	$C_{76}H_{60}Cl_2In_2O_8P_4Pd_2$ - 4 acetone
CCDC	990577	990578	990579	990580
Mol. Wt.	897.23	909.13	1635.76	1970.77
Crystal system	Monoclinic	Triclinic	Monoclinic	Triclinic
Space group	$P2_1/n$	$P\bar{1}$	$C2$	$P\bar{1}$
a/Å	12.644(1)	12.393(2)	22.608(2)	11.116(1)
b/Å	16.798(2)	13.325(2)	13.568(1)	19.005(2)
c/Å	17.833(2)	13.465(2)	13.497(1)	20.826(2)
α/°		96.11(1)		100.09(1)
β/°	104.01(1)	112.09(1)	116.15(1)	103.19(1)
γ/°		97.42(1)		99.94(1)
V/Å^3	3675.0(7)	2013.8(5)	3716.4(5)	4112.3(7)
Z	4	2	2	2
Calcd. density (g cm^{-3})	1.622	1.499	1.462	1.592
Abs. coeff. (mm^{-1})	1.430	0.617	0.780	1.188
F(000)	1816	936	1660	1984
Crystal size (mm)	0.20 x 0.12 x 0.08	0.16 x 0.08 x 0.04	0.12 x 0.06 x 0.02	0.18 x 0.09 x 0.03
θ range (°)	2.94 to 25.02	2.98 to 25.00	3.00 to 25.02	2.93 to 25.03
R(int)	0.087	0.124	-	0.072
Reflections measured	26201	28365	6509	43026
Unique reflections	6417	7058	6509	14483
Unique reflections[$I > 2\sigma(I)$]	4380	4608	4126	8938
Completeness to θ	99.2 %	99.6 %	99.8 %	99.6 %
Absorption correction	Semi-empirical from equivalents	Semi-empirical from equivalents	Semi-empirical from equivalents	Semi-empirical from equivalents
Max. and min. transmission	0.8620 and 0.7504	0.9801 and 0.6572	0.9801 and 0.7985	0.9703 and 0.8188
Data/restraints/parameters	6417 / 0 / 471	7058 / 37 / 520	6509 / 1 / 412	14483 / 224 / 981
Goodness of fit on F^2	1.07	1.04	0.95	1.02
R_1 ($I > 2\sigma(I)$)	0.053	0.076	0.070	0.057
$wR(F^2)$ (all data)	0.088	0.180	0.148	0.124
Largest diff. (e Å^{-3})	0.586 and -0.550	1.125 and -0.724	0.759 and -0.661	1.637 and -1.016
Flack parameter			-0.10(5)	

a) use of SQUEEZE (see ESI and cif-files)

Acknowledgements

We thank the Deutsche Forschungsgemeinschaft (DFG, grant Gu 415/12-1) for financial support and the Academy of Finland for a Research Fellowship. We further thank K. Wohlbold and J. Trinkner for measurement of mass spectra.

Notes and references

[a] Institut für Anorganische Chemie, University of Stuttgart, Pfaffenwaldring 55, 70550 Stuttgart, Germany. Fax: +49 711 685 64186 E-mail: gudat@iac.uni-stuttgart.de.

[b] Laboratory of Inorganic and Analytical Chemistry, University of Helsinki, P.O. Box 55 (A.I. Virtasen aukio 1), FIN-00014 Helsinki, Finland.

Electronic Supplementary Information (ESI) available: Cif-files, selected NMR spectra of **7** and **8**. See DOI: 10.1039/b000000x/

1 Selected reviews: a) L.-C. Liang, *Coord. Chem. Rev.* **2006**, *250*, 1152; b) F. Boeda, C. Beneyton, C. Crevisy, *Mini-Rev. Org. Chem.* **2008**, *5*, 96; c) J. I van der Vlugt, J. N. H. Reek, *Angew. Chem. Int. Ed. Engl.* **2009**, *48*, 8832; d) J. Wassenaar, J. N. H. Reek, Org. *Biomolec. Chem.*

2011, *9*, 1704; e) S. Lühr, J. Holz, A. Börner, *ChemCatChem* **2011**, *3*, 1708.

2 Selected reviews: a) W. Malisch, B. Klupfel, D. Schumacher, M. Nieger, *J. Organomet. Chem*. **2002**, *661*, 95; b) T. V. RajanBabu, Y.-Y.Yan, S. Shin, *Curr. Org. Chem*. **2003**, *7*, 1759; c) A. Börner, in *Aqueous-Phase Organometallic Catalysis* (Eds.: B. Cornils, W. A. Herrmann), Wiley-VCH, Weinheim **2004**, 2nd Ed., pp. 187; d) J. Heinicke, N. Peulecke, M. Köhler, M. He, W. Keim, *J. Organomet. Chem*. **2005**, *690*, 2449; e) M.-N. Gensow, A. Börner, *Multiphase Homogeneous Catalysis*, **2005**, *1*, 89; f) V. Andrushko, A. Börner, *Phosphorus Ligands in Asymmetric Catalysis* **2008**, *2*, 633.

3 a) X. Sun, D. W. Johnson, D. L. Caulder, R. Powers, K. N. Raymond E. H. Wong, *Angew. Chem. Int. Ed*. **1999**, *38*, 1303; b) X. Sun, D. W. Johnson, D. L. Caulder, R. E. Powers, K. N. Raymond E. H. Wong, *J. Am. Chem. Soc*. **2001**, *123*, 2752.

4 G. Bauer, D. Förster, M. Nieger, D. Gudat, *Z. Anorg. Allg. Chem*. **2014**, *640*, 325.

5 S. Chikkali, D. Gudat, F. Lissner, M. Niemeyer, Th. Schleid, M. Nieger, *Chem. Eur. J*. **2009**, *15*, 482.

6 S. H. Chikkali, M. Nieger, D. Gudat, *New J. Chem*. **2010**, *34*, 1348.

7 a) S. H. Chikkali, D. Gudat, F. Lissner, M. Nieger, T. Schleid, *Dalton. Trans.* **2007**, 35, 3906; b) G. Bauer, Z. Benkö, M. Nieger, J. Nuss, D. Gudat, *Chem. Eur. J*. **2010**, *16*, 12091.

8 G. Bauer, PhD Thesis, Stuttgart 2013.

9 R. D. Shannon, *Acta Crystallogr., Sect. A* **1976**, *32*, 751.

10 E. L. Muetterties, J. L. Guggenberger, *J. Am. Chem. Soc*. **1974**, *96*, 1748.

11 S. Alvarez, *Dalton Trans*. **2013**, *42*, 8617.

12 E. J. Bierschenk, N. R. Wilk, T. P. Hanusa, *Inorg. Chem.* **2011**, *50*, 12126.

13 Selected references: a) A. V. Piskunov, A. V. Maleeva, G. K. Fukin, E. V. Baranov, O. V. Kuznetsova, *Russian J. Coord. Chem*. **2010**, *36*, 161; b) V. Kriegisch, C. Lambert, *Eur. J. Inorg. Chem*. **2005**, 4509; c) S. Giroux, S. Aury, P. Rubini, S. Parant, J.-R. Desmurs, M. Dury, *Polyhedron* **2004**, *23*, 2393; d) M. H. Chisholm, J. Gallucci, D. Navarro-Llobet, H. Zhen, *Polyhedron* **2003**, *22*, 557; e) W. Ziemkowska, *Main Group Met. Chem*. **2000**, *23*, 337; f) S. N. Mhatre, S. B. Karweer, P. Pradhan, R. K. Iyer, P. N. Moorthy, *Dalton Trans*. **1994**, 3711; g) T. Kiss, K. Atkari, M. Jezowska-Bojczuk, P. Decock, *J. Coord. Chem*. **1993**, *29*, 81; h) T. B. Karpishin, T. D. P. Stack, i) K. N. Raymond, *J. Am. Chem. Soc*. **1993**, *115*, 182; j) E. W. Meijer, *Polyhedron* **1987**, *6*, 525.

14 G. M. Sheldrick, *Acta Crystallogr., Sect. A* **2008**, *64*, 112.

15 a) A. L. Spek, *Platon, A Multipurpose Crystallographic Tool*, Utrecht University, Utrecht, The Netherlands, **2004**; b) A. L. Spek, *Acta Crystallog.* **2009**, *D65*, 148.

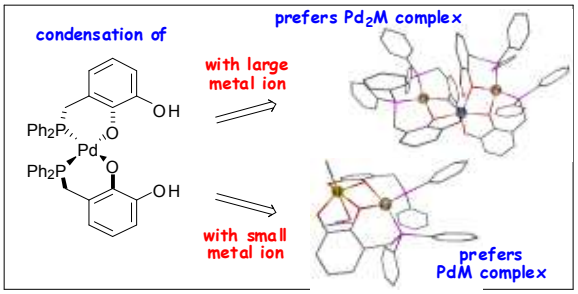

Condensation of a catechol phosphine Pd complex $[Pd(catphosH)_2]$ with group-13 element acetylacetonates yields heterometallic complexes $[M(L)_n(catphos)_2Pd]$ or $[M\{(catphos)_2Pd\}_2]H$ (M = Al, Ga, In) whose relative stability is controlled by the size of the group-13 element. ^1H NMR studies give insight into the proton mobility in $[In\{(catphos)_2Pd\}_2]H$.